Z boson pair production at CERN LHC in a stabilized Randall-Sundrum scenario

Seong Chan Park and H. S. Song
Department of Physics, Seoul National University, Seoul 151-742, Korea

Jeonghyeon Song
School of Physics, Korea Institute for Advanced Study, Seoul 130-012, Korea

(Received 3 April 2001; published 21 March 2002)

We study the Z boson pair production at the CERN Large Hadron Collider in the Randall-Sundrum (RS) scenario with the Goldberger-Wise stabilization mechanism. It is shown that a comprehensive account of the Kaluza-Klein (KK) graviton and radion effects is crucial to probe the model: The KK graviton effects enhance the cross section of $gg \to ZZ$ on the whole so that the resonance peak of the radion becomes easy to detect, whereas the RS effects on the $q\bar{q} \to ZZ$ process are rather insignificant. The p_T and invariant-mass distributions are presented to study the dependence of the RS model parameters. The production of longitudinally polarized Z bosons, to which the standard model contributions are suppressed, is mainly due to KK gravitons and the radion, providing one of the most robust methods to signal the RS effects. The 1σ sensitivity bounds on (Λ_π, m_ϕ) with $k/M_{\rm Pl}=0.1$ are also obtained such that the effective weak scale Λ_π of order 5 TeV can be experimentally probed.

DOI: 10.1103/PhysRevD.65.075008 PACS number(s): 11.30.Pb, 11.30.Er

I. INTRODUCTION

Recent advances in string theories have inspired particle physicists to approach the gauge hierarchy problem of the standard model (SM) in a very novel way, i.e., by introducing extra dimensions. Arkani-Hamed, Dimopoulos, and Dvali (ADD) proposed that there exist n large extra dimensions with factorizable geometry, whereas the SM fields are confined to our four-dimensional world [1]. The observed largeness of the Planck scale $M_{\rm Pl}$ is attributed to the large volume of the extra dimensions V_n, as can be seen from the relation $M_{\rm Pl}^2 = M_S^{n+2} V_n$ with M_S being the fundamental scale. Since M_S can be maintained around the TeV scale, the hierarchy problem is answered. Criticism arose because the ordinary gauge hierarchy is replaced by a new hierarchy between M_S and the compactification scale $\mu_c = V_n^{-1/n}$. Based on two branes and a single extra dimension with a nonfactorizable geometry, Randall and Sundrum (RS) proposed another higher dimensional scenario where, without a *large* volume of the extra dimension, the hierarchy problem is solved by a geometrical exponential factor [2]. Here the stabilization of the compactification radius is crucial, otherwise the study of the cosmological evolution in the RS scenario has shown that a nontrivial relationship between the matter densities on the two branes is required, which induces nonconventional cosmologies [3]. Goldberger and Wise (GW) have proposed a stabilization mechanism where a bulk scalar field with interactions localized on the two branes can generate for the modulus field a potential that allows a minimum appropriate to the hierarchy problem [4].

Of great interest and significance is that the ADD and RS models could possibly be detected at future collider experiments. Even more interestingly, they provide possible explanations for the recently reported deviation of the muon anomalous magnetic moment from the SM prediction [5,6]. In the ADD case, even though the coupling of each Kaluza-Klein (KK) graviton state with the SM fields is suppressed by the Planck scale, summation over the almost continuous KK spectrum compensates for the suppression and leaves an effective coupling of $\sim 1/M_S$ [7]. In the RS scenario, the zero mode of the KK graviton states couples with the usual Planck strength, whereas the masses and couplings of all the excited KK states are characterized by some electroweak scale Λ_π [8,9]. This discrete spectrum will yield a clean signal of graviton resonance production. Another key ingredient of the RS model comes from the stabilization mechanism, the radion. Since the radion can be much lighter than Λ_π [10–12], it is likely that the first signal of the RS effects will come from the radion.

Various phenomenological aspects of the radion have been extensively studied in the literature. The decay modes of the radion are different from those of the Higgs boson (e.g., the radion, with mass smaller than $2m_Z$, predominantly decays into two gluons) [10–12]; without a curvature-scalar Higgs mixing, the radion effects on the oblique parameters of the electroweak precision observations are small [11]. The radion effects on the phenomenology at low energy colliders [13] and at high energy colliders [14–16] have also been discussed.

In the RS scenario, however, there is another key ingredient, the KK spectrum of gravitons. Especially at a high energy collider, the comprehensive effects of the radion and KK gravitons can be substantial. Moreover, in spite of its lighter mass than the KK gravitons, the coupling strength of the radion with the SM particles is weaker than that of the KK gravitons for the following reasons: The characteristic scale of the radion coupling, inversely proportional to the vacuum expectation value (VEV) of the radion (Λ_ϕ), is smaller than the coupling of the KK gravitons, since $\Lambda_\phi = \sqrt{6}\,\Lambda_\pi$ [10]; the degrees of freedom of the spin-0 radion are less than those of the spin-2 massive KK gravitons. The Λ_ϕ, usually treated as a free parameter, is also constrained

 ©2002 The American Physical Society

through the relation with the Λ_π, which receives various constraints from the CERN e^+e^- collider LEP II and Fermilab Tevatron experiments [8]. We will show that the comprehensive consideration at high energy colliders leads to different phenomenologies from those with the radion effects only.

In order to sensitively probe the radion effects, we consider the process $gg \to ZZ$. Note that the radion interacts with the SM fields through the trace of the energy-momentum tensor: The coupling becomes stronger as the interacting SM particles are more massive, and the QCD trace anomaly enhances the coupling of the radion to a pair of gluons. This process has been extensively studied with special attention to the Higgs boson search at the CERN Large Hadron Collider (LHC) [17]. The double leptonic decay of the Z boson, $gg \to ZZ \to l^+l^-l'^+l'^-$, generates a clean signal. Unfortunately the main background of continuum production of the Z pair via $q\bar{q}$ annihilation is known to be dominant except in a limited range of the Higgs boson resonance. For example, full one-loop calculations for $gg \to ZZ$ in the minimal supersymmetric standard model (MSSM) with the squark loop contributions have shown that the irreducible background of $q\bar{q} \to ZZ$ surpasses even the resonant peaks of supersymmetric Higgs bosons [18].

As will be shown, comprehensive consideration of both KK graviton and radion effects is crucial to explore the RS model. The RS effects on the gluon fusion process are much larger than those on the $q\bar{q}$ process, which will be shown in the p_T and invariant-mass distributions. As a result, the radion effects on $gg \to ZZ$ have much more chance to be detected, while the radion effects on $q\bar{q} \to ZZ$ are negligible due to the smallness of m_q. Moreover, measurement of the Z polarization will provide another efficient method for probing the effects of the RS model.

This paper is organized as follows. In Sec. II, we briefly review the RS model with the GW mechanism, and summarize the effective Lagrangian between the KK graviton, the radion, and the SM particles. Model parameters are carefully defined. In Sec. III, the parton level helicity amplitudes for $gg \to ZZ$ and $q\bar{q} \to ZZ$ to leading order are given. In Sec. IV, we present numerical results for the p_T and invariant-mass distributions. After presenting the RS model dependence on the distributions, we will show the RS effects on various configurations of the Z-boson polarization. The sensitivity bounds for the parameter space of Λ_π and the radion mass are given. Finally, Sec. V deals with a summary and conclusions.

II. STABILIZED RANDALL-SUNDRUM SCENARIO

For the hierarchy problem, Randall and Sundrum proposed a five-dimensional nonfactorizable geometry with the extra dimension compactified on an S_1/Z_2 orbifold of radius r_c. Reconciled with four-dimensional Poincaré invariance, the RS configuration has the following solution to Einstein's equations:

$$ds^2 = e^{-2kr_c|\varphi|}\eta_{\mu\nu}dx^\mu dx^\nu + r_c^2 d\varphi^2, \tag{1}$$

where $0 \leqslant |\varphi| \leqslant \pi$ and k is the AdS_5 curvature. Two orbifold fixed points accommodate two three-branes, the hidden brane at $\varphi = 0$ and our visible brane at $|\varphi| = \pi$. The arrangement of our brane at $|\varphi| = \pi$ causes the fundamental scale m_0 to appear as the four-dimensional physical mass $m = e^{-kr_c\pi}m_0$. The hierarchy problem can be answered if $kr_c \approx 12$. From the four-dimensional effective action, the relation between the four-dimensional Planck scale $M_{\rm Pl}$ and the fundamental string scale M_S is obtained as

$$M_{\rm Pl}^2 = \frac{M_S^3}{k}(1 - e^{-2kr_c\pi}). \tag{2}$$

The compactification of the fifth dimension leads to the following four-dimensional effective Lagrangian [8]:

$$\mathcal{L} = -\frac{1}{M_{\rm Pl}}T^{\mu\nu}h_{\mu\nu}^{(0)} - \frac{1}{\Lambda_\pi}T^{\mu\nu}\sum_{n=1}^{\infty} h_{\mu\nu}^{(n)}, \tag{3}$$

where $\Lambda_\pi \equiv e^{-kr_c\pi}M_{\rm Pl}$ is at the electroweak scale. The coupling of the zero mode of the KK gravitons is suppressed by the usual Planck scale, and that of the massive KK gravitons by the electroweak scale Λ_π. The masses of the KK gravitons are also at the electroweak scale, given by [8,9]

$$m_n = kx_n e^{-kr_c\pi} = \frac{k}{M_{\rm Pl}}\Lambda_\pi x_n, \tag{4}$$

where the x_n's are the nth roots of the first order Bessel function. The condition $k < M_{\rm Pl}$ is to be imposed to maintain the reliability of the RS solution in Eq. (1) [19]. We take the value in the conservative range of $0.1 < k/M_{\rm Pl} < 0.7$. Then, the first excited KK graviton has a mass slightly larger than 1 TeV for $\Lambda_\pi \sim 3$ TeV and so there might be a chance to see the effects of KK gravitons at future high energy colliders.

In the original RS scenario, the compactification radius r_c is assumed to be constant. According to the studies of cosmological evolution, however, two branes want to blow apart, i.e., $r_c \to \infty$, unless we impose a fine-tuning between the densities on the two branes, which will lead to nonconventional cosmologies [3]. A stabilization mechanism is required. Goldberger and Wise have introduced a bulk scale field with the bulk mass somewhat smaller than k. The assumption of localizing the bulk scalar interactions on the two branes determines the four-dimensional effective potential for the radion, which can allow the minimum for $kr_c \approx 12$ without extreme fine-tuning. Furthermore, the radion mass is roughly an order of magnitude below Λ_π [13].

It was shown that the radion couples to ordinary matter through the trace of the symmetric and conserved energy-momentum tensor with TeV scale suppressed coupling:

$$\mathcal{L} = \frac{1}{\Lambda_\phi}\phi\, T_\mu^\mu, \tag{5}$$

where Λ_ϕ, the VEV of the radion field, is related such that $\Lambda_\phi = \sqrt{6}\,\Lambda_\pi$ [10]. The coupling of the radion with a fermion or massive gauge boson pair is the same as that of the Higgs boson, except for a factor of (v/Λ_ϕ), with v being the VEV

of the SM Higgs boson. The massless gluons and photons also contribute to T^{μ}_{μ}, due to the trace anomaly, which appears as the scale invariance of massless fields is broken by the running of gauge couplings [20]. Thus the interaction Lagrangian between two gluons and the radion or Higgs boson is

$$\mathcal{L}_{h(\phi)\text{-}g\text{-}g}=\left[\left(\frac{v}{\Lambda_{\phi}}\right)\{b_3+I_{1/2}(z_t^{\phi})\}\phi+I_{1/2}(z_t^{h})h\right] \times\frac{\alpha_s}{8\pi v}\ \mathrm{Tr}(G^C_{\mu\nu}G^{C\mu\nu}), \tag{6}$$

where $z_t^{\phi(h)}=4m_t^2/m^2_{\phi(h)}$, m_t is the top quark mass, and the QCD beta function coefficient is $b_3=11-2n_f/3$ with the number of dynamical quarks n_f. The loop function $I_{1/2}(z)$ is defined by

$$I_{1/2}(z)=z[1+(1-z)f(z)], \tag{7}$$

where $f(z)$ is

$$f(z)=\begin{cases}\arcsin^2(1/\sqrt{z}), & z\geqslant 1,\\ -\frac{1}{4}\left[\ln\left(\frac{1+\sqrt{1-z}}{1-\sqrt{1-z}}\right)-i\pi\right]^2, & z<1.\end{cases} \tag{8}$$

It is to be noted that the phenomenology of radions and KK gravitons in the RS model can be determined by three parameters, m_{ϕ}, Λ_{π}, and k/M_{Pl}.

III. Z BOSON PAIR PRODUCTION AT THE CERN LHC

A. The $gg\to ZZ$ helicity amplitudes

For the process $g(\lambda_1)g(\lambda_2)\to Z(\lambda_3)Z(\lambda_4)$ there are, in general, 36 helicity amplitudes corresponding to two and three polarization states of the initial gluons and final Z bosons, respectively. Various symmetry arguments reduce these 36 amplitudes to eight independent ones [17]. Parity invariance implies

$$\mathcal{M}_{\lambda_1\lambda_2\lambda_3\lambda_4}=\mathcal{M}^*_{-\lambda_1-\lambda_2-\lambda_3-\lambda_4}. \tag{9}$$

Bose statistics and the standard form of the Z-boson polarization vectors demand

$$\mathcal{M}_{++--}(\beta)=\mathcal{M}_{++++}(-\beta), \tag{10}$$

$$\mathcal{M}_{+++-}(\beta)=\mathcal{M}_{++-+}(\beta), \tag{11}$$

$$\mathcal{M}_{+---}(\beta)=\mathcal{M}_{+-++}(\beta), \tag{12}$$

$$\mathcal{M}_{+--+}(\beta)=\mathcal{M}_{+-+-}(-\beta), \tag{13}$$

$$\begin{aligned}\mathcal{M}_{+++0}(\beta)&=\mathcal{M}_{++0+}(\beta)\\&=\mathcal{M}_{++-0}(-\beta)\\&=\mathcal{M}_{++0-}(-\beta),\end{aligned} \tag{14}$$

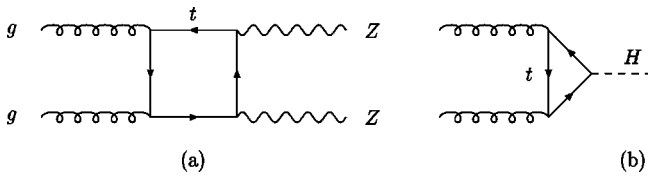

FIG. 1. Feynman diagrams for the process $gg\to ZZ$ in the SM.

$$\begin{aligned}\mathcal{M}_{+--0}(\beta)&=-\mathcal{M}_{+-0+}(-\beta)\\&=\mathcal{M}_{+--0}(-\beta)\\&=-\mathcal{M}_{+-0-}(\beta).\end{aligned} \tag{15}$$

For the explicit calculations, we consider the following four momenta for the initial gluons and final Z bosons in the gluon-gluon center-of-momentum (c.m.) frame:

$$p_1=\frac{\sqrt{\hat{s}}}{2}(1,0,0,1),\quad p_2=\frac{\sqrt{\hat{s}}}{2}(1,0,0,-1), \tag{16}$$

$$p_3=\frac{\sqrt{\hat{s}}}{2}(1,\beta\sin\theta,0,\beta\cos\theta),$$

$$p_4=\frac{\sqrt{\hat{s}}}{2}(1,-\beta\sin\theta,0,-\beta\cos\theta),$$

where $\beta=\sqrt{1-4m_Z^2/\hat{s}}$ and $\hat{t}=(p_1-p_3)^2$. The polarization vectors for the spin-1 particles with momentum $p^{\mu}=(p^0,\vec{p})$ are

$$\epsilon^{\mu}(p,\lambda)=\frac{e^{i\lambda\phi_{\hat{p}}}}{\sqrt{2}}(0,-\lambda\cos\theta\cos\phi_{\hat{p}}+i\sin\phi_{\hat{p}}, -i\cos\phi_{\hat{p}}-\lambda\cos\theta\sin\phi_{\hat{p}},\lambda\sin\theta), \tag{17}$$

$$\epsilon^{\mu}(p,0)=(|\vec{p}|/m,p^0\hat{p}/m), \tag{18}$$

where the angles θ and $\phi_{\hat{p}}$ specify the direction of $\vec{p}$.

In the SM, there are two types of Feynman diagram for the $gg\to ZZ$ process, through the box and triangle quark loops shown in Fig. 1. Despite loop suppression by a factor of α_s^2, the high luminosity of the gluon in a proton at the LHC yields a substantial cross section for the process. The SM helicity amplitudes have been studied in detail. We refer the reader to Ref. [17].

In the RS model, KK gravitons mediate the s-channel Feynman diagram at tree level (see Fig. 2). The helicity am-

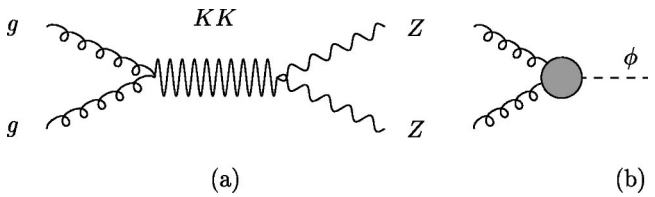

FIG. 2. Feynman diagrams for the process $gg\to ZZ$ mediated by (a) KK gravitons and (b) the radion in the RS model.

plitudes are cast into the form

$$\mathcal{M}^{G}_{\lambda_1\lambda_2\lambda_3\lambda_4}(gg\to ZZ)=-\frac{1}{8\Lambda_\pi^2}\sum_n \frac{\delta^{ab}}{\hat{s}-m_n^2}\mathcal{A}_{\lambda_1\lambda_2\lambda_3\lambda_4}, \tag{19}$$

where δ^{ab} denotes the color factor. There are six nonvanishing independent helicity amplitudes:

$$\mathcal{A}_{++++}=-\frac{1}{2}(\beta^4-1)(\hat{t}-\hat{u})^2+\frac{1}{2}(\beta^2+1)\hat{s}^2+(\hat{t}+\hat{u})\hat{s}, \tag{20}$$

$$\mathcal{A}_{+-+-}=\frac{1}{2}\{\beta(\hat{t}-\hat{u})+\hat{s}\}^2, \tag{21}$$

$$\mathcal{A}_{+-++}=\frac{1}{2}(\beta^2-1)\{\beta^2(\hat{t}-\hat{u})^2-\hat{s}^2\}, \tag{22}$$

$$\mathcal{A}_{+-+0}=-\frac{\sqrt{\hat{s}}}{2\sqrt{2}m_Z}(1-1/\beta^2)(\hat{t}-\hat{u}+\beta\hat{s})\times\sqrt{(\beta\hat{s})^2-(\hat{t}-\hat{u})^2}, \tag{23}$$

$$\mathcal{A}_{++00}=\frac{(1+\beta^2)\{(1+\beta^2)\hat{s}+2(\hat{t}+\hat{u})\}\hat{s}^2}{8m_Z^2}, \tag{24}$$

$$\mathcal{A}_{+-00}=\frac{(1-1/\beta^2)(\beta^2-2)\{(\hat{t}-\hat{u})^2-\beta^2\hat{s}^2\}\hat{s}}{8m_Z^2}. \tag{25}$$

The second ingredient of the RS model, the radion, couples to two gluons through its Yukawa coupling to a quark inside a triangle loop diagram, as well as through the QCD trace anomaly. Since the radion interaction with quarks is proportional to the mass, only the top quark loop needs to be considered. Two of the eight independent helicity amplitudes receive nonvanishing contributions from the radion:

$$\mathcal{M}^{\phi}_{++++}=-\frac{\alpha_s\delta^{ab}}{\pi}[b_{QCD}+I(z_t)]\left(\frac{m_Z}{\Lambda_\phi}\right)^2\times\frac{1}{\hat{s}-m_\phi^2+i\Gamma_\phi m_\phi}\frac{\hat{s}}{2}, \tag{26}$$

$$\mathcal{M}^{\phi}_{++00}=-\frac{\alpha_s\delta^{ab}}{\pi}[b_{QCD}+I(z_t)]\left(\frac{m_Z}{\Lambda_\phi}\right)^2\times\frac{1}{\hat{s}-m_\phi^2+i\Gamma_\phi m_\phi}\frac{\hat{s}^2(\beta^2+1)}{8m_Z^2}.$$

B. The $q\bar{q}\to ZZ$ helicity amplitudes

In the SM the process $q\bar{q}\to ZZ$ surpasses the gluon fusion process due to the presence of tree-level Feynman diagrams. Accurate structure functions at low x and higher order QCD corrections are necessary to obtain the precise ratio of the $q\bar{q}$ annihilation and gluon fusion processes. Even though the K factor of $\mathcal{O}(30\%)$ of $q\bar{q}\to ZZ$ is known [21], the absence of the corresponding calculation for the gluon fusion process leads us not to include any higher order corrections. We also assume that the uncertainties in leading contributions from soft gluon emission in both processes cancel to some extent in the ratio of cross sections, hardly affecting our main interest, the distribution shapes.

In the SM, there are t- and u-channel Feynman diagrams. Since the radion coupling to fermions is proportional to the fermion mass, we can safely neglect the radion effects here. The s-channel diagram mediated by KK gravitons, which is similar to the diagram (a) in Fig. 2, still influences the production. For the process $q(\lambda_1)\bar{q}(\lambda_2)\to Z(\lambda_3)Z(\lambda_4)$, the helicity amplitudes due to KK gravitons are written as

$$\mathcal{M}^{G}_{\lambda_1\lambda_2\lambda_3\lambda_4}(q\bar{q}\to ZZ)=-\frac{1}{4\Lambda_\pi^2}\sum_n \frac{\delta^{\alpha\beta}}{\hat{s}-m_n^2}\mathcal{B}_{\lambda_1\lambda_2\lambda_3\lambda_4}, \tag{27}$$

where the nonzero and independent $\mathcal{B}$'s are, in the parton c.m. frame,

$$\mathcal{B}_{+-++}=\frac{\hat{s}(\hat{t}-\hat{u})(\beta^2-1)\sin\theta}{\beta}, \tag{28}$$

$$\mathcal{B}_{+-+-}=\frac{\hat{s}(\hat{t}-\hat{u}+\beta\hat{s})\sin\theta}{\beta},$$

$$\mathcal{B}_{+-+0}=-\frac{(\beta^2-1)\hat{s}^{3/2}(1+\cos\theta)\{\beta\hat{s}-2(\hat{t}-\hat{u})\}}{2^{3/2}m_Z\beta},$$

$$\mathcal{B}_{+--+}=\hat{s}^2\sin\theta(\cos\theta-1),$$

$$\mathcal{B}_{+--0}=-\frac{(\beta^2-1)\hat{s}^{3/2}(1-\cos\theta)[\beta\hat{s}+2(\hat{t}-\hat{u})]}{2^{3/2}m_Z\beta},$$

$$\mathcal{B}_{+-00}=\frac{\hat{s}^2(\beta^2-1)(\beta^2-2)(\hat{t}-\hat{u})\sin\theta}{4m_Z^2\beta},$$

where $\cos\theta=(\hat{t}-\hat{u})/\beta\hat{s}$.

IV. CONTINUUM Z BOSON PAIR PRODUCTION AT THE CERN LHC

The physical production rate of Z boson pairs at pp colliders is obtained by convoluting over the parton structure functions [22]:

$$\sigma(pp\to ij\to ZZ)=\int dx_1\,dx_2\sum_{i,j} f_i(x_1,Q^2)f_j(x_2,Q^2)\hat{\sigma}_{ij}(x_1x_2s), \tag{29}$$

where i and j denote a parton such as a gluon or quark, and x_1 and x_2 denote the momentum fraction of the parton from the parent proton beam. For the numerical analysis, we use the leading order Martin-Roberts-Stirling-Thorne (MRST) parton distribution functions [23]. The QCD factorization and renormalization scales Q are set to be m_Z. The Q^2 dependence effect is expected to be small on the distribution shapes. The c.m. energy at the LHC is $\sqrt{s}=14$ TeV. We have employed the kinematic cuts of $p_T \geqslant 25$ GeV and $|\eta| \leqslant 2.5$ throughout the paper. As discussed before, the RS effects are determined by three parameters $(\Lambda_\pi, k/M_{\rm Pl}, m_\phi)$. From the above arguments, we consider $\Lambda_\pi = 2,3,5$ TeV, $k/M_{\rm Pl}=0.1,0.3,0.7$, and $m_\phi = 300,500,700$ GeV.

The SM Higgs boson mass has not been experimentally confirmed yet. Recently, the ALEPH group reported the observation of an excess of 3σ in the search for the SM Higgs boson, which corresponds to a Higgs boson mass about 114 GeV [24]. As the operation of LEP II has been completed, the decision whether the observations are only the results of statistical fluctuations or the first signal of Higgs boson production is suspended until the Tevatron II and/or LHC is running [25]. In the following, the Higgs boson mass is set to be 114 GeV except for the comparison of the contributions from the Higgs boson and radion with the same mass in Fig. 3.

Before presenting numerical results, some discussion of the unitarity violation of the RS model is in order here. As can be seen in the effective Lagrangian of Eqs. (3) and (5), the RS model generically undergoes unitarity violation at high energies $\sqrt{\hat{s}} \gg \Lambda_\pi$. In Ref. [6], the elastic process $\gamma\gamma \to \gamma\gamma$ was examined to obtain the bound from partial wave unitarity on the ratio $\sqrt{\hat{s}}/\Lambda_\pi$ in the RS model. This process can yield very sensitive bounds since the RS effects mediated by KK gravitons are dominant due to the absence of SM contributions. The J partial wave amplitude is defined [26] by

$$a^J_{\mu\mu'} = \frac{1}{64\pi}\int_{-1}^{1} d\cos\theta\, d^J_{\mu\mu'}(\cos\theta)[-i\mathcal{M}_{\lambda_1\lambda_2\lambda_3\lambda_4}], \tag{30}$$

where $\mathcal{M}_{\lambda_1\lambda_2\lambda_3\lambda_4}$ are the helicity amplitudes, $\mu=\lambda_1-\lambda_2$, $\mu'=\lambda_3-\lambda_4$, and $d^J_{\mu\mu'}$ are the Wigner functions [27]. Unitarity implies that the largest eigenvalue (χ) of $a^J_{\mu\mu'}$ is to be $|\chi|\leqslant 1$. The reliability of perturbative calculations is approximately guaranteed by the conditions $|\chi|=1$ and $|\mathrm{Re}(\chi)|=1/2$. The helicity amplitudes, of which the dominant contribution at high energies comes from the KK gravitons, are

$$\mathcal{M}_{++++} = \mathcal{M}_{----} = -i\,\frac{s^2}{\Lambda_\pi^2}\sum_n [D_n(t)+D_n(u)], \tag{31}$$

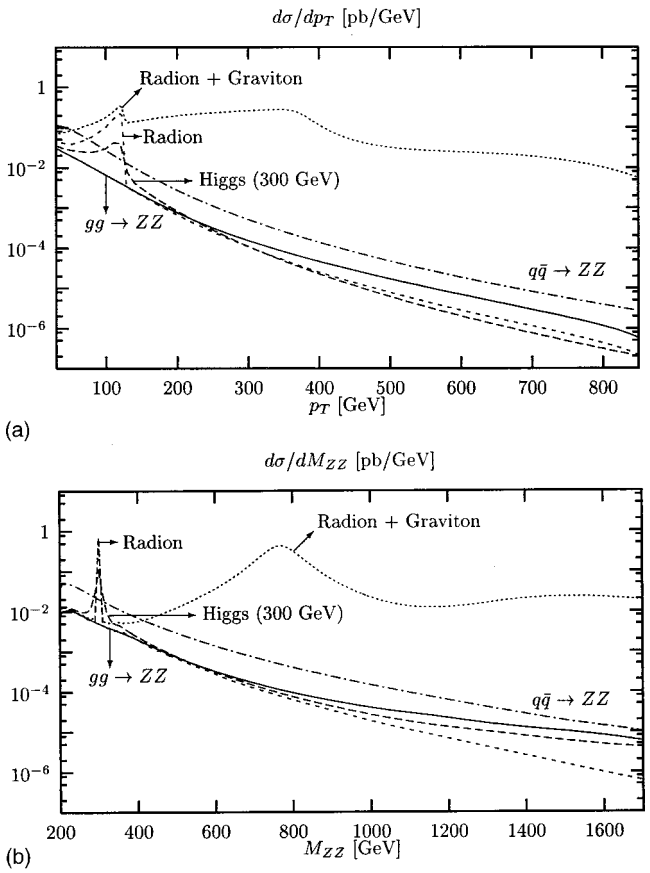

FIG. 3. The p_T and invariant-mass distributions of the $gg \to ZZ$ process when both the SM Higgs boson and radion masses are 300 GeV with $\Lambda_\pi = 2$ TeV and $k/M_{\rm Pl}=0.1$. The SM results for $q\bar{q}\to ZZ$ are plotted for comparison.

$$\mathcal{M}_{+--+} = \mathcal{M}_{-++-} = -i\,\frac{u^2}{\Lambda_\pi^2}\sum_n [D_n(s)+D_n(t)],$$

$$\mathcal{M}_{+-+-} = \mathcal{M}_{-+-+} = -i\,\frac{t^2}{\Lambda_\pi^2}\sum_n [D_n(s)+D_n(u)],$$

where $D_n(s)=1/(s-m_n^2+im_n\Gamma_n)$. The odd J partial wave amplitudes vanish due to Bose-Einstein statistics in elastic $\gamma\gamma$ scattering, and we have $a^2_{22}=a^2_{-2-2}$ and $a^2_{-22}=a^2_{2-2}$ from parity arguments. The nonvanishing eigenvalues χ_i are a^2_{00} and $2a^2_{22}$. Numerical estimation leads to $\sqrt{s}\lesssim 3.1\Lambda_\pi$ for $k/M_{\rm Pl}=0.1$, $\sqrt{s}\lesssim 5.7\,\Lambda_\pi$ for $k/M_{\rm Pl}=0.3$, and $\sqrt{s}\lesssim 9.8\,\Lambda_\pi$ for $k/M_{\rm Pl}=0.7$. In what follows, a very conservative bound is employed, such as $\sqrt{\hat{s}}\leqslant 0.9\Lambda_\pi$. In order to eliminate the concern about unitarity violation, it is reasonable that we restrict ourselves to the region where our perturbative calculations are trustworthy. This can be achieved by excluding data with high invariant mass. In the following, therefore, we constrain the invariant mass to be less than 1.8 TeV, to be consistent with our parametrizations of Λ_π.

First we present the p_T and invariant-mass distributions for unpolarized Z bosons. Figure 3 shows the effects of the radion and KK graviton for the process $gg\to ZZ$ on the dis-

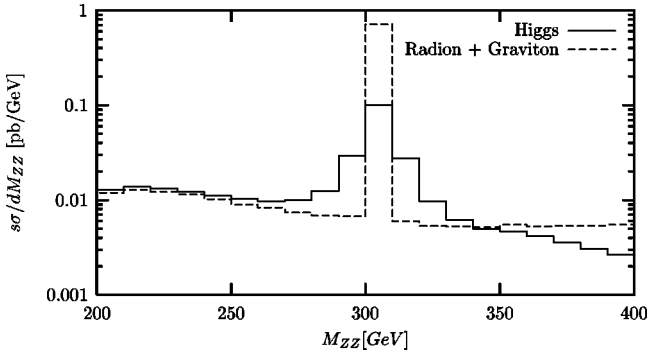

FIG. 4. The resonance peak shapes in the invariant-mass distributions of the $gg \to ZZ$ process when both the SM Higgs boson and radion masses are 300 GeV with $\Lambda_\pi = 2$ TeV and $k/M_{\rm Pl} = 0.1$.

tributions. For comparison, both the Higgs boson and radion masses are set to be 300 GeV with $\Lambda_\pi = 2$ TeV and $k/M_{\rm Pl} = 0.1$. The long dashed line denotes the SM results with the Higgs boson mass of 300 GeV. The short dashed line includes only the radion effects, whereas the dotted line incorporates both the KK graviton and radion effects. The SM result for $q\bar{q} \to ZZ$ denoted by the dash-dotted line is also plotted for comparison. The p_T distributions apparently show that the KK graviton effects enhance the cross section on the whole, which increases the chance to probe for the presence of the radion. Other models for new physics beyond the SM,

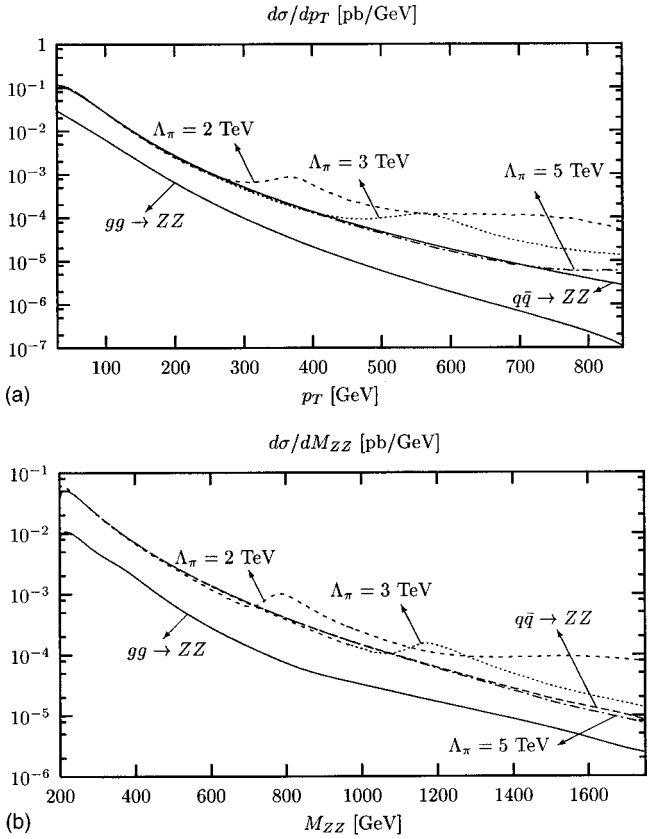

FIG. 5. The p_T and invariant-mass distributions of the $q\bar{q} \to ZZ$ process for $\Lambda_\pi = 2$, 3, and 5 TeV. The SM results for $gg \to ZZ$ are plotted for comparison.

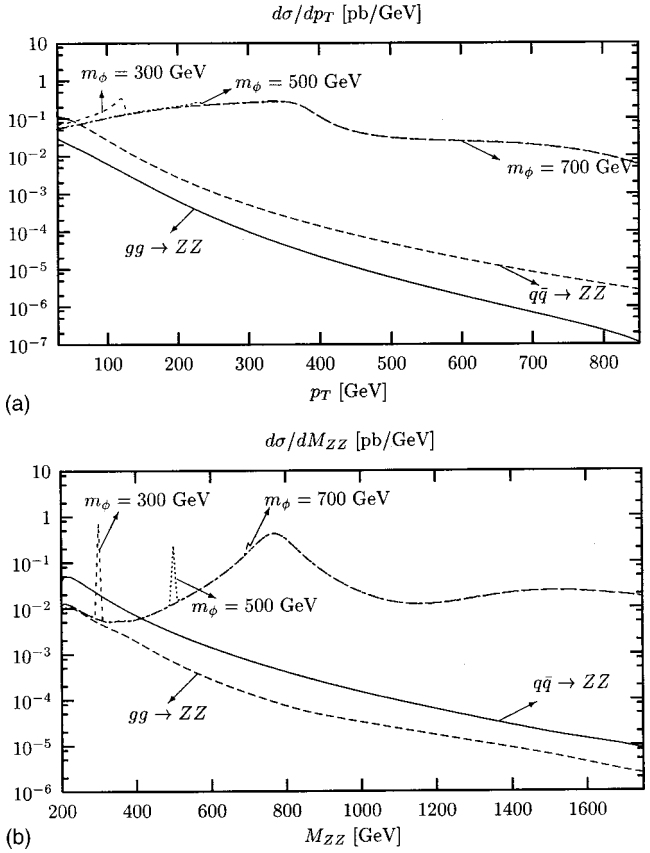

FIG. 6. The p_T and invariant-mass distributions of the $gg \to ZZ$ process for $m_\phi = 300$, 500, and 700 GeV with $\Lambda_\pi = 2$ TeV and $k/M_{\rm Pl} = 0.1$. The SM results for $q\bar{q} \to ZZ$ are plotted for comparison.

including supersymmetric models, do not generate such elevated resonance behavior. Even in the large Λ_π case where the KK graviton effects are negligible, distinction between the Higgs boson and radion is, in principle, possible: The resonance peak of the radion becomes narrower with increasing Λ_π because the radion total decay width (Γ_ϕ) is inversely proportional to Λ_π^2. Figure 4 shows the resonance shapes of the Higgs boson and radion with the same mass, through the invariant mass spectrum of the Z pair. It can be seen that if both have the same mass the radion shows a sharper resonance peak than the Higgs boson. This is generic since the total decay width of the radion is smaller than that of the Higgs boson due to the radion's larger VEV.

In Fig. 5, we present the RS effects on the process $q\bar{q} \to ZZ$, which are determined solely by the Λ_π due to the ignorance of the radion influence. The KK gravitons can be recognized by broad peaks. The RS effects are less important than those on the $gg \to ZZ$ process: The effects appear beyond 300 GeV of p_T and 700 GeV of M_{ZZ}, generating at most 10^{-3} pb/GeV of the differential cross section with respect to p_T or M_{ZZ}; the effects on gluon fusion will be shown to appear in the low p_T and M_{ZZ} region where the cross sections are sizable.

Now we illustrate the dependence of the gluon fusion process on each parameter of the RS model. In Fig. 6, we plot

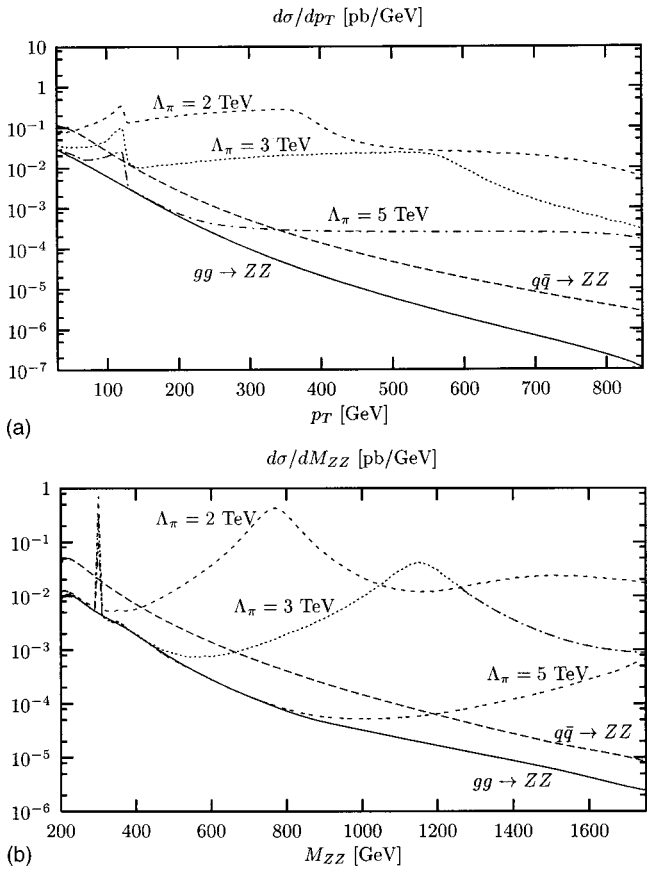

FIG. 7. The Λ_π dependence of the p_T and invariant-mass distributions of the $gg \to ZZ$ process for $\Lambda_\pi = 2$, 3, and 5 TeV with $m_\phi = 300$ GeV and $k/M_{\rm Pl} = 0.1$.

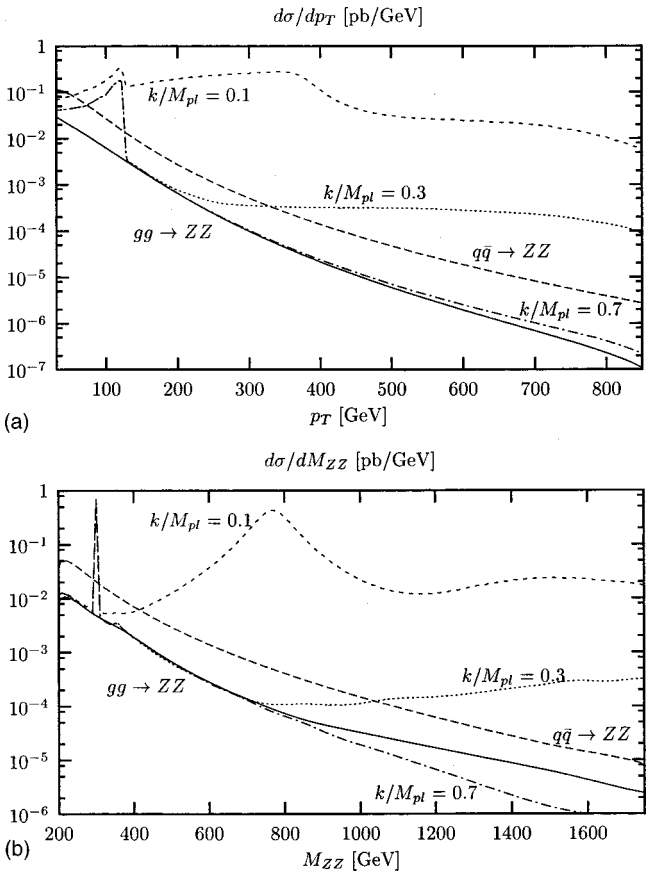

FIG. 8. The $k/M_{\rm Pl}$ dependence of the p_T and invariant-mass distributions of the $gg \to ZZ$ process for $k/M_{\rm Pl} = 0.1$, 0.3, and 0.7 with $m_\phi = 300$ GeV, and $\Lambda_\pi = 2$ TeV.

the distributions for $m_\phi = 300,500,700$ GeV, with $\Lambda_\pi = 2$ TeV and $k/M_{\rm Pl} = 0.1$. It can be seen that the resonance peak of lighter radions is sharper. If the radion is quite heavy (around 500 GeV in this parameter space), the contribution of the KK gravitons to the p_T distributions overwhelms the radion resonance; it is more appropriate to probe the invariant-mass distribution. If the radion is too heavy (more than 700 GeV in this case), large contributions of the KK gravitons obscure the radion effects. Figure 7 presents the Λ_π dependence of the $gg \to ZZ$ process for $\Lambda_\pi = 2$, 3, and 5 TeV with $m_\phi = 300$ GeV and $k/M_{\rm Pl} = 0.1$. The M_{ZZ} distributions show a sharp resonance peak of the radion and successive broad peaks of the KK gravitons. In the p_T distributions, the KK graviton effects yield a plateau region. The case of $\Lambda_\pi \gtrsim 5$ TeV would be difficult to probe. The $k/M_{\rm Pl}$ dependence is presented in Fig. 8, for $k/M_{\rm Pl} = 0.1$, 0.3, and 0.7 with $m_\phi = 300$ GeV and $\Lambda_\pi = 2$ TeV. Since $k/M_{\rm Pl}$ is proportional to the masses of the KK gravitons [see Eq. (4)], the KK graviton effects in the large $k/M_{\rm Pl}$ cases are hardly detected. Note that in the RS model the magnitude of the five-dimensional curvature ($R_5 = -20k^2$) is required to be smaller than M_S^2 ($\simeq M_{\rm Pl}^2$) for reliability of the classical RS solution derived from the leading order term in the curvature. A value of $k/M_{\rm Pl}$ less than about 0.1 is theoretically favored [19].

We present the influence of the Z polarization measurement on the distributions. Figures 9 and 10 are for the polarization states $Z_T Z_T$ and $Z_L Z_L$, respectively. We set $\Lambda_\pi = 2$ TeV, $k/M_{\rm Pl} = 0.1$, and $m_\phi = 300$ GeV for illustration. As expected from the scalar nature of the radion and the spin-2 nature of massive KK gravitons, longitudinally polarized Z bosons are produced more in the RS model, while the SM production of $Z_L Z_L$ through both gluon fusion and $q\bar{q}$ annihilation is suppressed. Thus measurement of the longitudinally polarized Z bosons would provide one of the most robust methods to single out, in particular, the radion effects of the RS model.

Unfortunately, an event cannot determine the polarization of the Z boson. The angular distributions for Z boson decay, $Z \to f\bar{f}$, provide some information on the Z polarization. To leading order, the RS effects can be ignored in Z decay. Neglecting the mass of the final state fermions, the angular distributions of the Z decay rate are given by, in the rest frame of the decaying Z [28],

$$\frac{1}{\Gamma_f}\frac{d\Gamma^\pm}{d\cos\chi} = \frac{3}{8}[\alpha_f(1 \mp \cos\chi)^2 + (1-\alpha_f)(1 \pm \cos\chi)^2] \tag{32}$$

for the transversely polarized Z bosons, and

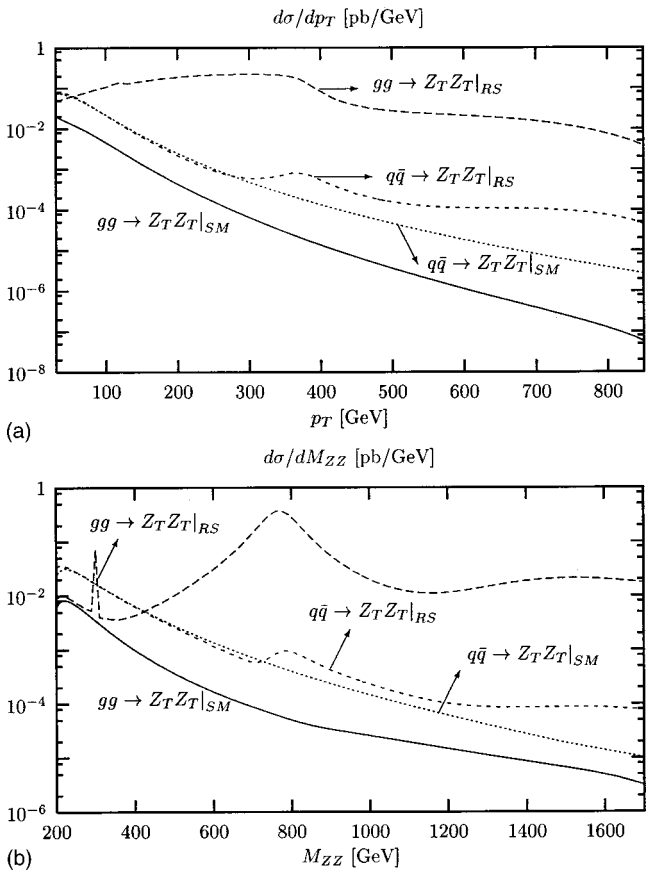

FIG. 9. The p_T and invariant-mass distributions of the $gg \to Z_T Z_T$ process. We set $k/M_{\rm Pl}=0.1$, $m_\phi=300$ GeV, and $\Lambda_\pi=2$ TeV.

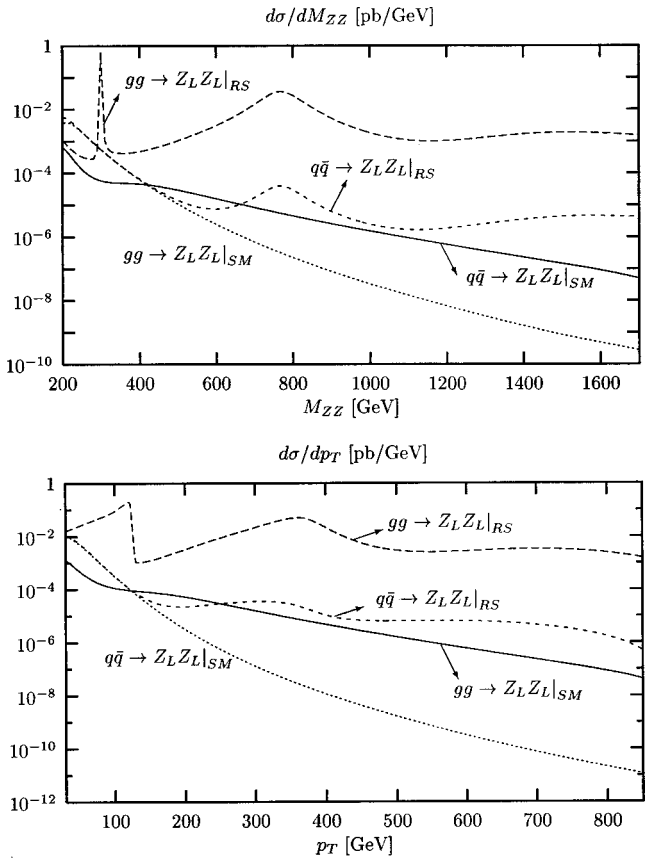

FIG. 10. The p_T and invariant-mass distributions of the $gg \to Z_L Z_L$ process. We set $k/M_{\rm Pl}=0.1$, $m_\phi=300$ GeV, and $\Lambda_\pi=2$ TeV.

$$\frac{1}{\Gamma_f}\frac{d\Gamma^0}{d\cos\chi}=\frac{3}{4}\sin^2\chi \tag{33}$$

for the longitudinally polarized Z bosons. For charged leptonic decay, we have $\alpha_f=(1-2x_W)^2/(1-4x_W+8x_W^2)$ with $x_W\equiv\sin^2\theta_W$. The partial width Γ_f is for the normalization, and χ is the angle between the fermion momentum direction and the spin axis as seen in the Z rest frame (the Z boost direction in the helicity basis). Therefore, an appropriate cut on χ would select more data of longitudinally polarized Z bosons. We define the ratio $\mathcal{R}$, which is proportional to the observable RS effects as follows:

$$\mathcal{R}\equiv\frac{\sigma(pp\to ZZ\to l^+l^-l'^+l'^-)_{SM+RS}}{\sigma(pp\to ZZ\to l^+l^-l'^+l'^-)_{SM}}, \tag{34}$$

where $l,l'=e,\mu,\tau$. In order to focus on the detection of radion effects, we employ a kinematic cut, e.g., $p_T<125$ GeV only for the estimates of $\mathcal{R}$. Numerical analysis shows that with the kinematic cut of $|\cos\chi|<0.3$ $\mathcal{R}$ increases by 49% with respect to the value without any cut on χ. Thus appropriate kinematic cuts on the transverse momentum of the Z boson and the angle χ can enhance the signal for the radion effects by, e.g., about 50%.

Finally, we estimate the 1σ search bounds on the Λ_π and the radion mass, which are obtained by comparing the *total* cross sections with and without the RS effects. Even though the cross section of longitudinally polarized Z bosons (σ_{LL}) and/or the radion resonance peak are powerful methods to probe the RS effects, higher sensitivity bounds, which are usually relevant in the case of no signal, are obtained from the observable with *larger* event number. As discussed before, the RS model has unitarity violation at high energies, which may induce unphysically large contributions to the total cross section. One possible way is to exclude data with high invariant mass, i.e., to employ an upper cut on M_{ZZ} such as $\sqrt{\hat{s}}\leqslant 0.9\Lambda_\pi$. Thus we require that

$$\frac{\sigma^<_{SM+RS}-\sigma^<_{SM}}{\sqrt{\sigma^<_{SM}}}\sqrt{\mathcal{L}}\,\epsilon\geqslant 1, \tag{35}$$

where $\sigma^<$ denotes the total cross section with an additional kinematic cut of $M_{ZZ}<900$ GeV. ϵ is the reconstruction efficiency for the Z boson pair, which is the squared branching ratio of the Z boson into e^+e^- or $\mu^+\mu^-$. The LHC luminosity $\mathcal{L}$ is 100 pb^{-1}. In Fig. 11, we show the attainable 1σ bounds on Λ_π and m_ϕ with $k/M_{\rm Pl}=0.1$. Even with restrictive efficiency, a Λ_π of about 5 TeV can be experimentally

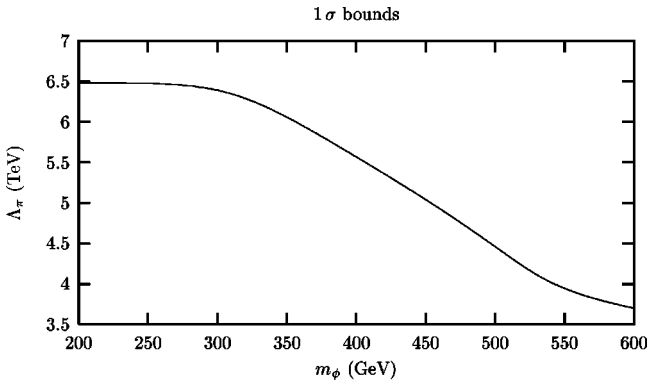

FIG. 11. The 1σ sensitivity bounds on (Λ_π, m_ϕ) with $k/M_{\rm Pl}=0.1$.

examined. Since the radion has a relatively small influence upon the total cross section, the p_T or invariant-mass distribution would be more appropriate to signal the radion effects.

V. SUMMARY AND CONCLUSION

We have studied the $gg\to ZZ$ process at the LHC as a probe of the Randall-Sundrum scenario with the Goldberger-Wise stabilization mechanism. Even though the process has been regarded as significant in various aspects (e.g., in examining the Higgs sector), the main background of continuum production of $q\bar{q}\to ZZ$ is known to be dominant in the SM and MSSM. It has been shown that the comprehensive effects of Kaluza-Klein gravitons and the radion enhance the chance to probe the model: The RS effects on the $q\bar{q}\to ZZ$ process, which are generated only by KK gravitons, are much smaller than those on $gg\to ZZ$; the KK graviton effects increase the cross section of $gg\to ZZ$ throughout the p_T and invariant-mass distributions; the resonance shape of the radion is distinguishable from that of the Higgs boson. Numerical results for the p_T and invariant-mass distributions have been obtained to show the dependence on the RS model parameters $(\Lambda_\pi, k/M_{\rm Pl}, m_\phi)$. Distinction between the Higgs boson and radion even with the same mass is feasible since the resonance peak of the radion is narrower than that of the Higgs boson in most of the parameter space. The p_T and invariant-mass distributions for the polarized Z boson pair have also been presented. We have shown that in particular the production of longitudinally polarized Z bosons, to which the SM contributions are suppressed, receives substantial corrections due to KK gravitons and the radion. Polarization measurements would provide one of the most robust methods to signal the RS effects. The 1σ sensitivity bounds on (Λ_π, m_ϕ) with $k/M_{\rm Pl}=0.1$ have also been obtained. Λ_π of about 5 TeV can be experimentally searched even with restrictive experimental efficiency. In conclusion, the channel of Z boson pair production at the LHC with measurement of the Z polarizations and the kinematic distributions can provide an efficient method to probe the effects of the RS scenario with the modulus fields being stabilized by the Goldberger-Wise mechanism.

ACKNOWLEDGMENTS

We would like to thank K. Y. Lee and W. Y. Song for useful discussions on this work. The work was supported by the BK21 Program.

[1] I. Antoniadis, N. Arkani-Hamed, S. Dimopoulos, and G. Dvali, Phys. Lett. B **436**, 257 (1998); N. Arkani-Hamed, S. Dimopoulos, and G. Dvali, *ibid.* **429**, 263 (1998).
[2] L. Randall and R. Sundrum, Phys. Rev. Lett. **83**, 3370 (1999).
[3] C. Csaki, M. Graesser, L. Randall, and J. Terning, Phys. Rev. D **62**, 045015 (2000).
[4] W.D. Goldberger and M.B. Wise, Phys. Rev. Lett. **83**, 4922 (1999); Phys. Lett. B **475**, 275 (2000).
[5] S.C. Park and H.S. Song, Phys. Lett. B **511**, 99 (2001).
[6] C.S. Kim, J.D. Kim, and J. Song, Phys. Lett. B **511**, 251 (2001).
[7] G.F. Giudice, R. Rattazzi, and J.D. Wells, Nucl. Phys. **B544**, 3 (1999); T. Han, J.D. Lykken, and R. Zhang, Phys. Rev. D **59**, 105006 (1999).
[8] H. Davoudiasl, J.L. Hewett, and T.G. Rizzo, Phys. Rev. Lett. **84**, 2080 (2000).
[9] W.D. Goldberger and M.B. Wise, Phys. Rev. D **60**, 107505 (1999).
[10] G.F. Giudice, R. Rattazzi, and J.D. Wells, Nucl. Phys. **B595**, 250 (2001).
[11] U. Mahanta and S. Rakshit, Phys. Lett. B **480**, 176 (2000).
[12] S.B. Bae, P. Ko, H.S. Lee, and J. Lee, Phys. Lett. B **487**, 299 (2000).
[13] C. Csaki, M.L. Graesser, and G.D. Kribs, Phys. Rev. D **63**, 065002 (2001).
[14] U. Mahanta and A. Datta, Phys. Lett. B **483**, 196 (2000); K. Cheung, Phys. Rev. D **63**, 056007 (2001).
[15] S.R. Choudhury, A.S. Cornell, and G.C. Joshi, hep-ph/0012043.
[16] K. Cheung, Phys. Rev. D **63**, 056007 (2001).
[17] E.W. Glover and J.J. van der Bij, Nucl. Phys. **B321**, 561 (1989).
[18] M.S. Berger and C. Kao, Phys. Rev. D **59**, 075004 (1999).
[19] H. Davoudiasl, J.L. Hewett, and T.G. Rizzo, Phys. Lett. B **473**, 43 (2000).
[20] J.C. Collins, A. Duncan, and S.D. Joglekar, Phys. Rev. D **16**, 438 (1977).
[21] V. Barger, J.L. Lopez, and W. Putikka, Int. J. Mod. Phys. A **3**, 2181 (1988).
[22] E. Eichten, I. Hinchliffe, K. Lane, and C. Quigg, Rev. Mod. Phys. **56**, 579 (1984); V. Barger, J.L. Lopez, and W. Putikka [21].
[23] A.D. Martin, R.G. Roberts, W.J. Stirling, and R.S. Thorne, Eur. Phys. J. C **14**, 133 (2000).
[24] ALEPH Collaboration, R. Barate *et al.*, Phys. Lett. B **495**, 1 (2000); L3 Collaboration, M. Acciarri *et al.*, *ibid.* **495**, 18

(2000); J. Ellis, G. Ganis, D.V. Nanopoulos, and K.A. Olive, *ibid.* **502**, 171 (2001); S.C. Park, H.S. Song, and J. Song, Phys. Rev. D **63**, 077701 (2001).
[25] J. Ellis, hep-ex/0011086.
[26] O.J. Eboli, T. Han, M.B. Magro, and P.G. Mercadante, Phys. Rev. D **61**, 094007 (2000).
[27] Particle Data Group Collaboration, D.E. Groom *et al.*, Eur. Phys. J. C **15**, 1 (2000).
[28] G. Mahlon and S. Parke, Phys. Rev. D **58**, 054015 (1998).